Proceedings of the Korean Nuclear Society Spring Meeting
Gyeongju, Korea, May 2004

Validation of GAMMA-3D Using Inverse U-tube and HTTR-Simulated Air Ingress Experiments

Hong Sik Lim
Korea Atomic Energy Research Institute
150 Dukjin-dong, Yuseong-gu, Taejon, Korea 305-353
hslim@kaeri.re.kr

Hee Cheon NO
Korea Advanced Institute of Science and Technology
373-1 Guseong-dong, Yuseong-gu, Taejon, Korea 305-701
hcno@nsys.kaist.ac.kr

Abstract

One of the key safety issues for HTGRs is the air ingress accident following a guillotine-type break at the coaxial pipe between the reactor vessel and the heat exchange system. We developed a multi-dimensional GAs Multicomponent Mixture Analysis (GAMMA) in order to investigate molecular diffusion, chemical reactions, and natural convection related to the air ingress phenomena during the primary-pipe rupture accident. In the simulations of both simplified inverse U-tube and HTTR-simulated air ingress experiments, the predicted results follow the experimental ones consistently regarding the concentration changes of each species and the onset times of natural convection show a level of agreement within a 10% deviation from the experimental data. Small internal leaks in the HTTR-simulated test facility have been found to significantly affect the consequence of air ingress.

1. Introduction

High Temperature Gas-Cooled Reactors (HTGR) are considered a future nuclear energy option by virtue of their high degree of inherent safety performance and very high temperature supply capability.

However, it is still unclear if the present HTGRs can maintain a passive safe function when the primary-pipe rupture accident, a guillotine-type break of the coaxial double pipe at the nozzle part connecting to the bottom of the reactor vessel, is postulated to occur. When the primary-pipe rupture accident happens, it is expected that air entering into a reactor vessel chemically reacts with the high temperature graphite components, causing the temperature of fuel elements to rise and the graphite components to be corroded. Therefore, it is necessary to confirm that the air ingress accident cannot seriously oxidize the graphite fuel elements to release the radioactive products from the reactor core to the environment nor severely damage the graphite components to loose the integrity of the reactor internals.

When the postulated guillotine break of the coaxial pipe happens, the high-pressure helium gas is discharged into the reactor container through the breach. After a few minutes, the gas pressure becomes balanced between the inside and outside of the reactor vessel. After the depressurization stage, it is supposed that air enters into the reactor core from the breach due to molecular diffusion and a weak natural convection induced by the distribution of gas temperature and the resulting concentrations in the reactor. Carbon monoxide (CO) and dioxide (CO_2) are produced in the reactor by chemical reactions between the oxygen (O_2) contained in air and the high temperature graphite structures. The density of the gas mixture in the reactor gradually increases in the first stage of the accident, and eventually the buoyancy force becomes substantial enough to overcome the gravitational force. Finally, the second stage of the accident starts after natural circulation of the air occurs suddenly throughout the entire reactor.

Although the occurrence frequency of this event is extremely low, the possibility of the catastrophic failures like graphite fire, CO detonation, and structural collapse must still be considered. In order to study this concern, basic experimental studies were performed using simplified U-shaped tube and HTTR-simulated test facilities in Japan. For the sake of understanding the basic phenomena and investigating the key mechanisms related to the air ingress accident, GAMMA has been validated with two kinds of air ingress experiments.

2. Governing Equations and Numerical Method

The multi-dimensional governing equations consist of the basic equations for continuity, momentum conservation, energy conservation of the gas mixture, and the mass conservation of each species. Six gas species (He, N_2, O_2, CO, CO_2, and H_2O) are considered. GAMMA has the capability to handle the thermal hydraulic and chemical reaction behaviors in a multicomponent mixture system as well as heat transfer within solid components, free and forced convection between solid and fluid, and radiation heat transfer between solid surfaces. As well, the basic equations are formulated with a porous media model to consider a pebble bed-type HTGR.

2.1 Governing Equations

The field equations used in GAMMA are:

Continuity equation

$$\varphi\frac{\partial\rho}{\partial t}+\nabla\cdot\left(\rho\mathbf{u}\right)=\varphi\sum_{s}R_{s} \tag{1}$$

Momentum equation in a non-conservative form

$$\rho\left(\frac{1}{\varphi}\frac{\partial\mathbf{u}}{\partial t}+\frac{1}{\varphi^{2}}\mathbf{u}\cdot\nabla\mathbf{u}\right)=-\nabla P+\frac{1}{\varphi}\nabla\cdot\left(\mu\nabla\mathbf{u}\right)-\frac{\mu}{K}\mathbf{u}-\frac{C_{F}\rho}{\sqrt{K}}\left|\mathbf{u}\right|\mathbf{u}+\rho\mathbf{g} \tag{2}$$

Sensible energy equation for the fluid

$$\varphi\frac{\partial}{\partial t}\left(\rho H\right)+\nabla\cdot\left(\rho\mathbf{u}H\right)=\nabla\cdot\left(\varphi\lambda_{f}\nabla T_{f}\right)-\nabla\cdot\left(\varphi\sum_{s=1}^{m}H_{s}\mathbf{J}_{s}\right)-\varphi\sum_{s}\Delta h_{f\,s}^{o}R_{s}+h_{sf}a_{sf}\left(T_{p}-T_{f}\right) \tag{3}$$

Species conservation equation

$$\varphi\frac{\partial}{\partial t}\left(\rho Y_{s}\right)+\nabla\cdot\left(\rho\mathbf{u}Y_{s}\right)=-\nabla\cdot\left(\varphi\mathbf{J}_{s}\right)+\varphi R_{s} \tag{4}$$

and for He, $Y_{m}=1-\sum_{s=1}^{m-1}Y_{s}$

Equation of state for an ideal gas

$$\rho=\frac{P}{\overline{R}T}\left(\sum_{s=1}^{m}Y_{s}/W_{s}\right)^{-1} \tag{5}$$

For a solid and a pebble bed, the same heat conduction equation is used. A thermal non-equilibrium model is used to consider the heat exchange between fluid and pebbles in porous medium as follows:

$$\left[\left(1-\varphi\right)\left(\rho C\right)_{p}\right]\frac{\partial T_{p}}{\partial t}=\nabla\cdot\left(\lambda_{eff}\nabla T_{p}\right)+q'''-h_{sf}a_{sf}\left(T_{p}-T_{f}\right) \tag{6}$$

The ordinary diffusion flux ($\mathbf{J}_s$) is given in two forms, full multicomponent diffusion [1] and effective diffusion [2] by assuming that a dilute species, s, diffuses through a homogeneous mixture:

$$\mathbf{J}_{s}=\rho\frac{W_{s}}{W^{2}}\sum_{k=1,k\neq s}^{m}\left[D_{sk}\nabla\left(Y_{k}W\right)\right]\quad\text{and}$$
$$\mathbf{J}_{s}=-\rho D_{s-mix}\nabla Y_{s}\quad where\ \ D_{s-mix}=\left(\sum_{k=1,k\neq s}^{m}X_{k}/\mathbf{D}_{sk}\right)^{-1}\ \ (\mathrm{m}\geq 3) \tag{7}$$

Physical properties, such as molar weight, viscosity, thermal conductivity, and sensible enthalpy, for each gas component and gas mixtures, are obtained from References 3 and 4.

2.2 Numerical Method

The governing equations are discretized in a semi-implicit manner in the staggered mesh layout and then dependent variables are linearized by the Newton method. For a fast computation, the Implicit Continuous Eulerian (ICE) technique [5] is adopted to reduce 10N×10N matrix to N×N pressure difference matrix. Due to the explicit treatment of the second order terms, GAMMA is subjected to restriction of time step size, limited by convective, diffusive, conductive, and viscous transport times. The heat conduction equation, Eq. (6), is solved by the Crank-Nicolson method and coupled explicitly in 3-D form or implicitly in 1-D form with the fluid thermal-hydraulic calculation.

3. Validation Results

The most important chemical reactions between oxygen and graphite are the following heterogeneous reactions:

A. $C + O_2 \rightarrow CO_2 + 3.935\times10^5$ (J/mole)
B. $C + (1/2)O_2 \rightarrow CO + 1.105\times10^5$ (J/mole)
C. $C + CO_2 \rightarrow 2CO - 1.725\times10^5$ (J/mole)

and the homogeneous reaction:

D. $CO + (1/2)O_2 \rightarrow CO_2 + 2.830\times10^5$ (J/mole).

A Dryer and Glassman's correlation [6] is used for the CO combustion (D) and our new correlation [7] for the IG-110 graphite oxidation (A and B). A Boudouard reaction (C) is not considered in the present calculation because a reaction rate for IG-110 is unavailable and the graphite temperatures in most test cases are relatively low.

3.1 Inverse U-tube Air Ingress Experiment

Figure 1 shows the GAMMA nodal scheme for the inverse U-tube experimental apparatus [8], which consisted of a gas tank and an inverse U-shaped tube with a graphite (IG-110) tube inserted at the middle of the hot side: an inverse U-shaped tube having an inner diameter of 40.5 mm connected to a gas tank of a height of 400 mm and a diameter of 991 mm. Initially air or nitrogen was filled in the gas tank and helium in the tube, respectively, and the high temperature side and connecting pipes were heated to the elevated temperatures. When the ball valves at the inlet of an inverse U-shaped pipe, nitrogen or air enters into the vertical pipe by molecular diffusion and weak natural convection.

As time passes, the density of the gas mixture in the hot side gradually increases but at a faster rate than in the cold pipe, and eventually global natural convection initiates. In the air-filled case, air transported from the tank chemically reacts with the graphite. As the graphite is oxidized by a chemical reaction with oxygen, CO and CO_2 are produced and transported both upward and downward. A part of the CO produced dissipates by a homogeneous reaction with oxygen, thus further producing an amount of CO_2.

Table 1 lists all test conditions conducted in the inverse U-tube system. Figure 2 shows the typical behavior of velocities at the tube inlets and the CO_2 produced, which are calculated for the test AS12. In the figure, the onset time of natural convection (OTNC) is clearly indicated between the first and second stages. A primary importance for the first stage is to predict the onset time of natural convection. As shown in Figure 3, even with some discrepancies in the concentrations of species, the predicted onset times of the natural convection show a level of agreement with those of the experiment, with a 3% deviation for the N_2-filled condition and about 6% for the air-filled condition, respectively. It is because the density change of the gas mixture is not highly sensitive to the concentrations of species. The initiation time of global natural convection is slightly reduced in the air-filled case due to production of heavier gases by chemical reaction, compared to the N_2-filled case.

3.2 HTTR-simulated Air Ingress Experiment

Figure 4 shows the HTTR-simulated experimental facility [8], which consisted of a reactor core simulator, a high-temperature plenum, a water-cooled jacket corresponding to the reactor vessel and simulated inlet and outlet pipes corresponding to the coaxial pipe. The reactor core simulator had four graphite tubes (one central and three peripherals) and a ceramic plenum. The graphite tube had an inner diameter of 40 mm and a height of 800 mm. Density of gas mixture and concentrations of O_2, CO, and CO_2 were measured at five sampling points indicated by the symbol, (⦿), in Figure 4.

First of all, a vertical slot test [9] was simulated to investigate the effect of local circulation on molecular diffusion, which is expected to occur in an annular passage of the HTTR-simulated system and thus affects the consequence of air ingress. The vertical slot system consists of a rectangular dimension of 720×290×820mm in a bottom tank and 20×956×590mm in a thin slot, each initially filled with only a He-air mixture and He, respectively. Since the width of the slot is relatively very thin compared to that of the tank, a 2-D geometry model can be used. Figure 5 shows that air ingress for the temperature difference of 5^oC is greatly promoted by local natural circulation compared to the pure diffusion case. The range of the Rayleigh number calculated based on the width of the slot is about $350 < Ra < 550$. Compared to the ideal calculation result, it seems that the flow field is distorted by non-uniform slot temperature distribution and rough surface conditions due to thermocouples attached on the inner surface of the slot thus lowering the air transport rate during the

experiment. GAMMA gives better predictions at the later stage than the FLUENT [10] does, because in GAMMA the depth is controlled simply thus preserving the fluid volume of each part.

The GAMMA nodal scheme for the HTTR-simulated system is shown in Figure 4. On the basis of previous investigation, an annular passage in the HTTR-simulated system is modeled by 2-D geometry to consider the effect of local natural circulation. Local natural circulation in other regions is much less important because it mixes gas components quickly. As a representative case among test cases listed in Table 2, the predicted results for the non-equal temperature case B8575 are shown in Figures 6 though 9. As time passes, oxygen is transported by molecular diffusion and weak natural convection toward both hot and cold sides. In particular, since local natural circulation in the annular passage promotes air transport into the top cover, graphite oxidation takes place in both bottom and top portions of the graphite tubes. We estimate that the range of the Rayleigh number is about $2\times10^4 < Ra < 2\times10^5$ based on the width of an annular passage, and local velocity is about 0.6 m/s, comparable to the velocity of global natural convection. As oxygen is consumed in the graphite tubes and the amount of heavy gases, CO and CO_2, produced by chemical reactions increases gradually, the buoyancy force induced by the distribution of the gas mixture becomes substantial enough to overcome a gravitational force. Eventually global natural convection is initiated through the entire test apparatus.

In the first calculation, we have found that the CO_2 produced at the bottom of graphite tubes is trapped in the hot plenum. Therefore, as shown in Figure 8, the predicted mole fractions of CO_2 are higher in the hot plenum but lower in the top cover and annular regions compared to those of the measured data, thus delaying the consequence of air ingress. The onset time of natural convection is delayed by around 1.5 days, corresponding to a deviation greater than 10%. Its delay is presumed to be caused by several leak paths, which are established directly as well as indirectly through the thermal insulator from the hot side to the cold side. The leak paths will affect the CO_2 distribution in a complicated manner. In the subsequent calculation, all the leak paths are modeled by single path with a very small area ($1.5\times10^{-5}m^2$); therefore, although exact leakage data are not given in the experiment report [8], a small leak path is considered as a natural process in all other calculations. Figure 10 shows that the onset times of natural convection for all test cases are accurately predicted within a 10% deviation.

4. Conclusions

For the simulation of the simplified inverse U-tube experiment, the predicted trends of concentration changes of each species follow the experimental data consistently and the predicted onset times of the natural convection agree closely with those of the experiment, with a 3% deviation for the N_2-filled condition and about 6% for the air-filled condition, respectively.

From the vertical slot simulation, it is confirmed that GAMMA is efficient to consider local natural circulation and preserve geometric volumes important for the conservation of partial mass.

By taking into account a small leak path as a natural process, the onset times of natural convection are predicted well within a 10% deviation for all test cases of the HTTR-simulated air ingress experiment. However, much simplification of complex leak paths slightly compromises the accuracy of the predictions of the concentration distribution of CO_2. Also, at high temperatures above 900°C, we need further experimentation to determine a reaction rate of the C-CO_2 reaction for IG-110 in order to get better prediction for the concentration changes of species.

Nomenclature

a_{sf} = specific surface area (m^{-1})
C_F = drag coefficient
D_{sk} = multicomponent diffusion coefficient (m^2/s)
$\mathbf{D}_{sk}$ = binary diffusion coefficient (m^2/s)
D_{s-mix} = effective diffusion coefficient (m^2/s)
g = gravitational constant
h_{sf} = interfacial heat transfer coefficient. (W/m^2-K)
Δh_f^o = latent heat of formation for chemical reaction (J/kg)
H = sensible enthalpy of gas mixture (J/kg)
H_s = sensible enthalpy of species, s (J/kg)
$\mathbf{J}_s$ = total diffusion flux w.r.t. mass average velocity (kg/m^2-s)
K = permeability
m = total number of species
N = total number of computational meshes
P = total pressure (Pa)
q''' = volumetric heat source (W/m^3)
$\bar{R}$ = universal gas constant
Ra = Rayleigh number
R_s = generation/dissipation of species, s, by chemical reaction (kg/m^3-s)
T_f = temperature of gas mixture (K)
T_p = solid or pebble temperature (K)
$\mathbf{u}$ = mass average velocity (m/s)
W = molar weight of gas mixture (g/mol)
W_s = molar weight of species, s (g/mol)
X_s = mole fraction of species, s

Y_s = mass fraction of species, s

Greek Symbols

ρ = density of gas mixture (kg/m^3)
$(\rho C)_p$ = volumetric heat capacity of solid or pebble (J/ m^3-K)
φ = porosity
λ_f = thermal conductivity of gas mixture (W/m-K)
λ_{eff} = effective thermal conductivity of solid or pebble bed (W/m-K)
μ = viscosity of gas mixture (kg/m-s)

References

[1] J.O. Hirschfelder, C.F. Curtiss, R.B. Bird, *Molecular Theory of Gases and Liquids*, Wiley, 1964.

[2] R.E. Walker, N. Dehaas, A.A. Westenberg, "Measurements of Multicomponent Diffusion Coefficients for the CO_2-He-N_2 System Using the Point Source Technique," *J. Chem. Phys*., Vol.32, No.5, p.1314, 1960.

[3] B.E. Poling, J.M. Prausnitz, J.P. O'connell, *The Properties of Gases and Liquids*, McGraw-Hill, 2001.

[4] K. Raznjevic, *Handbook of Thermodynamic Tables and Charts*, Hemisphere, Washington, 1976.

[5] F.H. Harlow, A.A. Amsden, "A Numerical Fluid Dynamics Calculation Method for All Flow Speeds," *J. Comp. Phy.*, Vol.8, p.197-213, 1971.

[6] F.L. Dryer, I. Glassman, "High-Temperature Oxidation of CO and H_2," *14th symposium (international) on combustion*, The Combustion Institute, Pittsburgh, p.987-1003, 1973.

[7] H.S. Lim, H.C. No, "Transient Multicomponent Mixture Analysis Based on ICE Numerical Scheme For Predicting an Air Ingress Phenomena in an HTGR," *The 10th International Topical Meeting on Nuclear Reactor Thermal Hydraulics (NURETH-10)*, October 2003.

[8] T. Takeda, *Air Ingress Behavior during a Primary-pipe Rupture Accident of HTGR*, JAERI-1338, 1997.

[9] T. Takeda, *Mixing Process of a Binary Gas in a Density Stratified Layer*, JAERI-Research97-061, 1997.

[10] *FLUENT 6.0 User's Guide*, FLUENT Inc., 2002.

Table 1. Experimental cases conducted in the inverse U-tube system

N_2-filled condition		Air-filled condition	
Run No.	Heated pipe temperature (^oC)	Run No.	Heated pipe temperature (^oC)
NS1	379.7	AS1	569.1
NS2	462.8	AS2	661.8
NS3	555.3	AS3	767.7
NS4	659.4	AS4	715.4
NS5	758.0	AS5	618.1
NS6	707.4	AS6	466.2
NS7	618.9	AS7	376.6
NS8	508.7	AS8	523.5
NS9	425.2	AS9	423.8
NS10[a]	367.3	AS10	16.3
-		AS12	811.0

Note: a. This case has different temperature distribution pattern from other tests.

b. No data given for the isothermal test AS11 (14.6^oC).

Table 2. Experimental cases conducted in the HTTR-simulated system

Equal Temperature condition		Non-equal Temperature condition	
Run No.	Central and peripheral graphite temperatures (^oC)	Run No.	Central and peripheral graphite temperatures (^oC)
A40	405.4 (108.8/20.3)[a]	B1090	994.1, 907.7 (214.4/25.0)
A60	607.8 (159.3/28.0)	B8575	847.8, 765.6 (180.9/26.6)
A70	708.2 (181.2/26.4)	B7060	697.6, 613.2 (136.3/15.2)
A75	756.9 (193.2/29.5)	B7060b	697.6, 619.2 (142.7/27.7)
A80	806.7 (195.9/29.6)	B4030	396.3, 329.6 (90.0/27.8)
A85	857.7 (220.5/37.2)		
A90	908.0 (225.4/33.2)		
A95	955.7 (247.0/44.6)		
A100	1002.7 (247.7/46.1)		
A105	1045.7 (270.1/53.6)		

Note: a. Core barrel and pressure vessel wall temperatures.

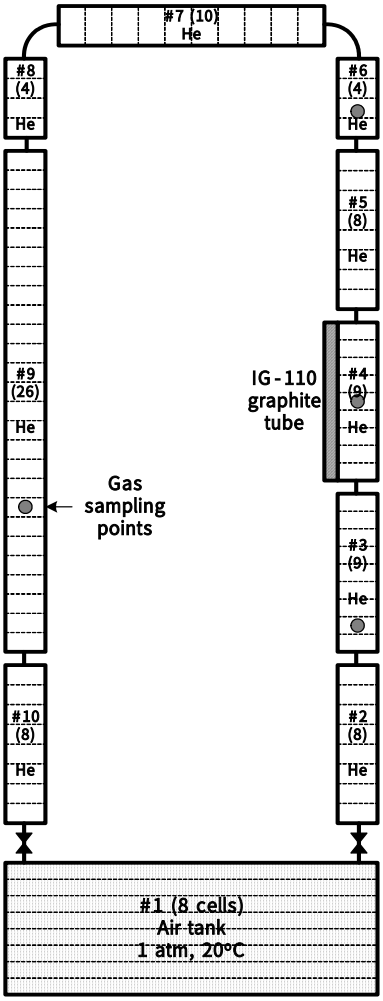

Fig. 1. GAMMA nodalizaion for the inverse U-tube system.

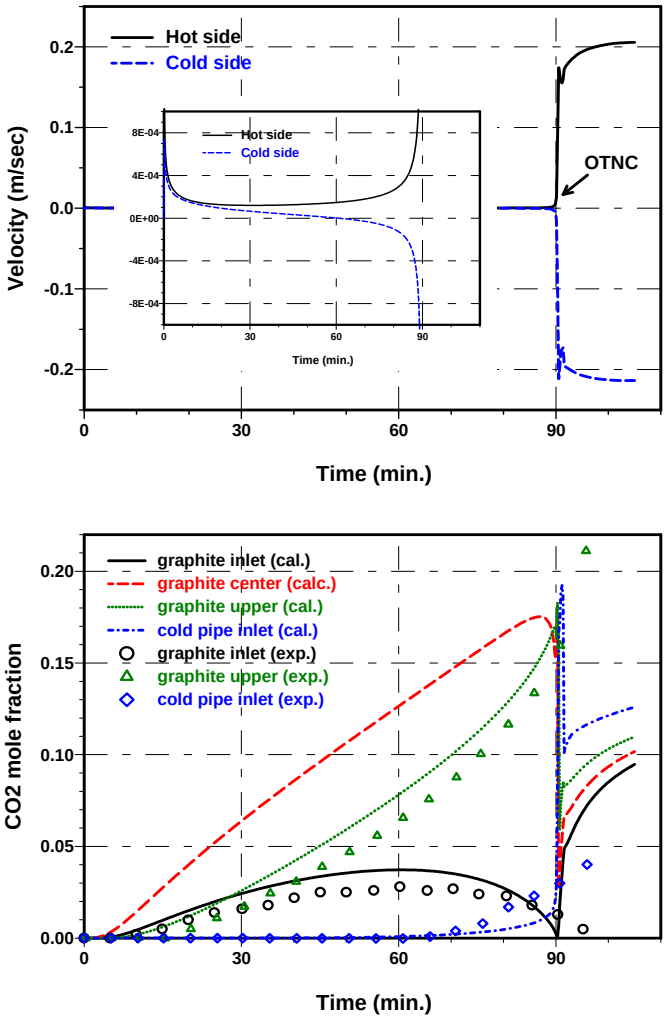

Fig. 2. Predicted velocities and mole fractions of dioxide for the test AS12.

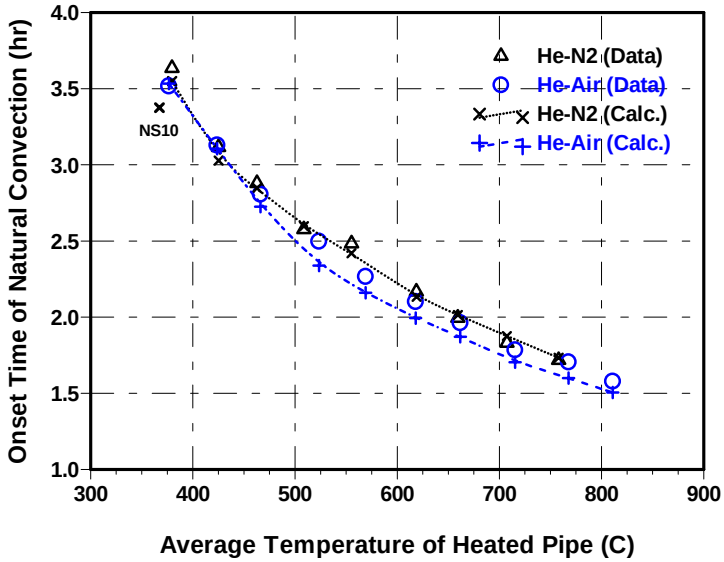

Fig. 3. Predicted onset times of natural convection (OTNC) for the inverse U-tube system.

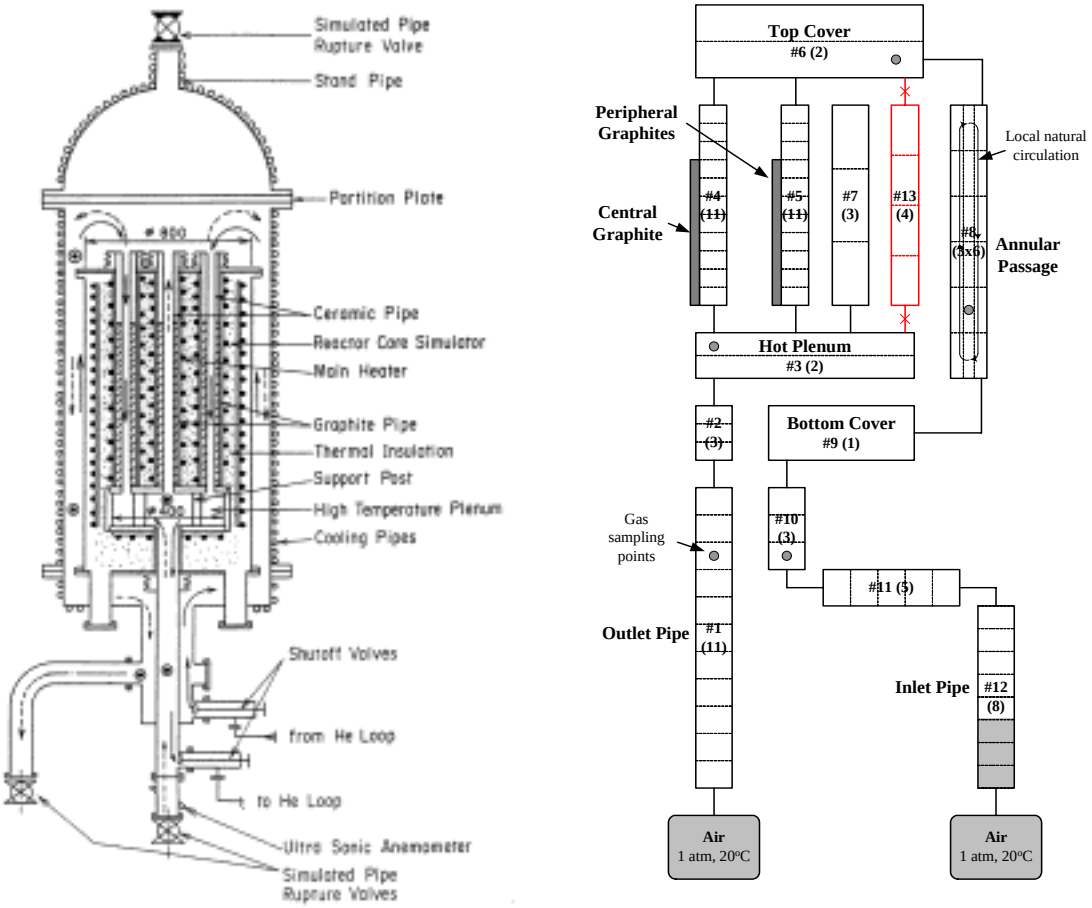

Fig. 4. Schematic diagram of the HTTR-simulated system and GAMMA nodalization.

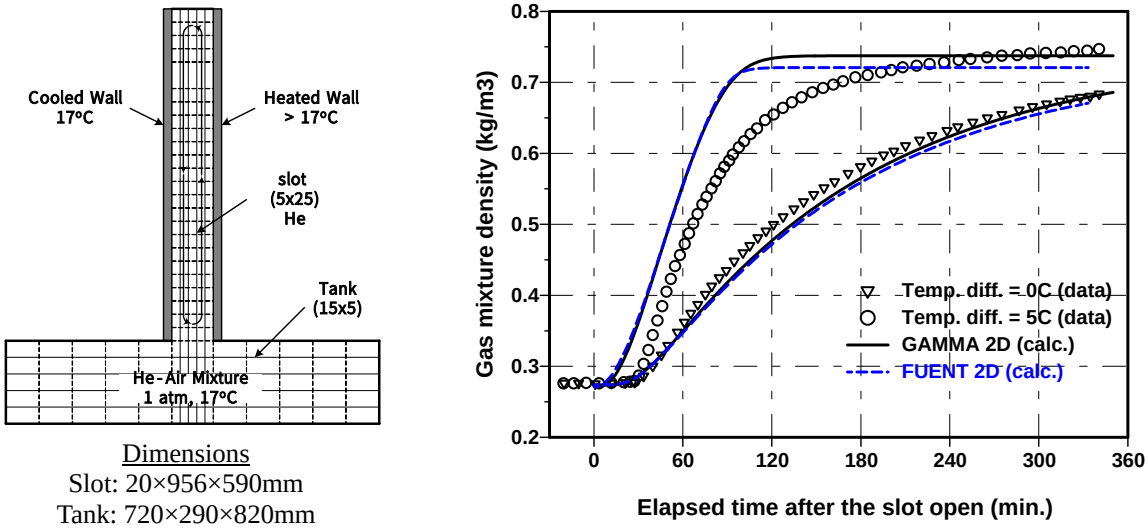

Dimensions
Slot: 20×956×590mm
Tank: 720×290×820mm

Fig. 5. 2-D calculation layout for the vertical slot system and predicted densities of gas mixture at the top of the slot.

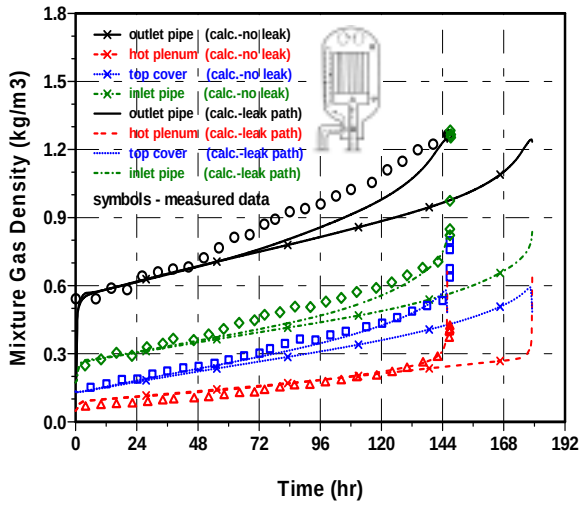

Fig. 6. Predicted densities of gas mixture

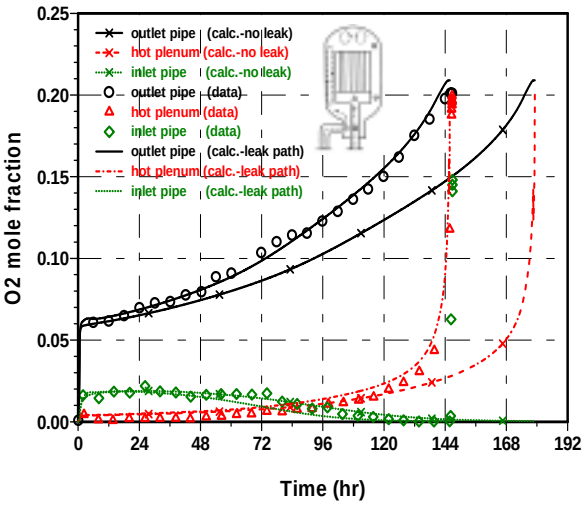

Fig. 7. Predicted mole fractions of oxygen

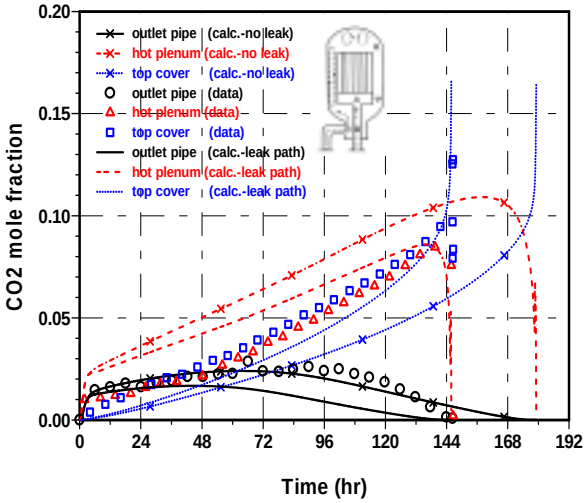

Fig. 8. Predicted mole fractions of dioxide

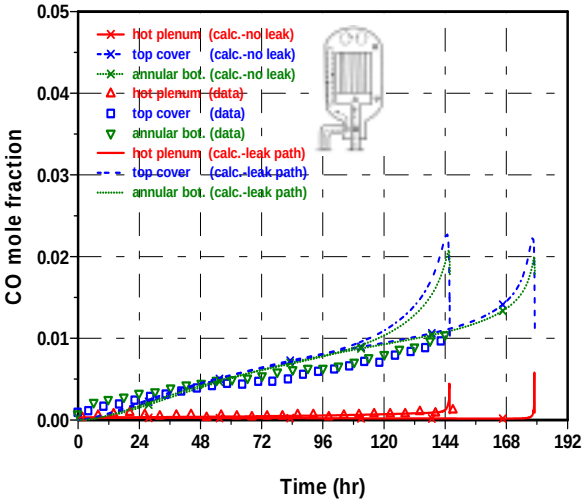

Fig. 9. Predicted mole fractions of monoxide

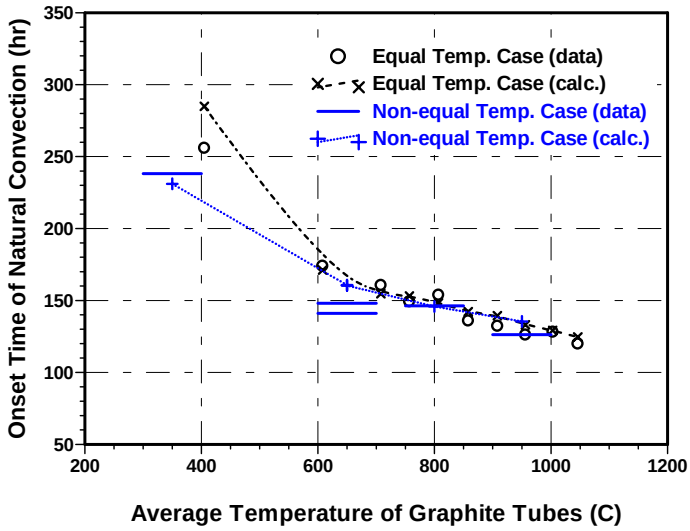

Fig. 10. Predicted onset times of natural convection (OTNC) for the HTTR-simulated system